Binding of ATP to the CBS domains in the C-terminal region of CLC-1

Pang-Yen Tseng,[1,2] Wei-Ping Yu,[1,2] Hao-Yang Liu,[3,4] Xiao-Dong Zhang,[1,2] Xiaoqin Zou,[3,4] and Tsung-Yu Chen[1,2]

[1]Center for Neuroscience and [2]Department of Neurology, University of California, Davis, Davis, CA 95618
[3]Department of Physics and [4]Department of Biochemistry, Dalton Cardiovascular Research Center, Informatics Institute, University of Missouri, Columbia, MO 65211

The common gating of CLC-1 has been shown to be inhibited by intracellular adenosine triphosphate (ATP) in acidic pH conditions. Such modulation is thought to be mediated by direct binding of ATP to the cystathionine β-synthase (CBS) domains at the C-terminal cytoplasmic region of CLC-1. Guided by the crystal structure of the C-terminal domain of CLC-5, we constructed a homology model of CLC-1's C terminus and mutated critical amino acid residues lining the potential ATP-binding site. The CLC-1 mutations V634A and E865A completely abolished the ATP inhibition of CLC-1, consistent with the loss of ATP binding seen with the corresponding mutations in CLC-5. Mutating two other residues, V613 and V860, also disrupted the ATP modulation of CLC-1. However, placing aromatic amino acids at position 634 increases the apparent ATP affinity. Mutant cycle analyses showed that the modulation effects of ATP and cytidine triphosphate on wild-type CLC-1 and the V634F mutant were nonadditive, suggesting that the side chain of amino acid at position 634 interacts with the base moiety of the nucleotide. The mutation effects of V634F and V613A on the ATP modulation were also nonadditive, which is consistent with the assertion suggested from the homology model that these two residues may both interact with the bound nucleotide. These results provide evidence for a direct ATP binding for modulating the function of CLC-1 and suggest an overall conserved architecture of the ATP-binding sites in CLC-1 and CLC-5. This study also demonstrates that CLC-1 is a convenient experimental model for studying the interaction of nucleotides/nucleosides with the CBS domain.

The Journal of General Physiology

INTRODUCTION

The resting conductance of the sarcolemma of skeletal muscles consists of a Cl^- component largely contributed by the CLC-1 Cl^- channel (Jentsch et al., 2002, 2005; Chen, 2005). It has been shown that the inhibition of the sarcolemmal Cl^- conductance is critical for reducing the shunting conductance and, therefore, for helping the muscle overcome fatigue resulting from the accumulation of extracellular K^+ ions after continuous firing of action potentials (Pedersen et al., 2004, 2005). This antifatigue mechanism is thought to result from the ATP inhibition of the common gating of CLC-1 in the presence of an acidic intracellular pH (Bennetts et al., 2007; Tseng et al., 2007). Presumably, ATP acts on the protonated CLC-1 channel by binding to the cystathionine β-synthase (CBS) domain located at the C-terminal cytoplasmic region (Meyer and Dutzler, 2006; Markovic and Dutzler, 2007; Meyer et al., 2007), although the molecular mechanism of the CLC-1 modulation by ATP appears to be unsettled. Although our study (Tseng et al., 2007) and that of Bennetts et al. (2005, 2007) demonstrated an ATP inhibition of the common gating of CLC-1, others have suggested that ATP may exert its actions on CLC-1 indirectly via an accessory protein (Zifarelli and Pusch, 2008). We have recently shown that the controversy may result from different degrees of oxidation of the CLC-1 channel molecule in various experimental conditions (Zhang et al., 2008). However, a study to provide evidence for a direct binding of ATP to the predictive ATP-binding site of CLC-1 is imperative.

So far, the high resolution structure of the C-terminal domain of CLC-1 is not available. However, the C-terminal structure is known in several CLC molecules, including CLC-0, CLC-Ka, CLC-5, and CmCLC (Meyer and Dutzler, 2006; Markovic and Dutzler, 2007; Meyer et al., 2007; Feng et al., 2010). All these C-terminal structures show conserved CBS domains. The CLC-5's C-terminal structure is particularly helpful because it is the only CLC structure in which the ATP molecule can be seen at the ATP-binding site in the CBS domain. Mutating two CLC5's amino acid residues that interact with the bound ATP, as guided by the x-ray structure, reduces the ATP binding affinity (Meyer et al., 2007). Based on the C-terminal domain of CLC-5, we constructed a homology model of the C terminus of CLC-1. We mutated several previously unexamined amino acid residues in CLC-1 that appear to interact with the bound ATP molecule.

Correspondence to Tsung-Yu Chen: tycchen@ucdavis.edu

Abbreviations used in this paper: CBS, cystathionine β-synthase; dATP, deoxy-ATP; WT, wild type.

The Rockefeller University Press $30.00
J. Gen. Physiol. Vol. 137 No. 4 357–368
www.jgp.org/cgi/doi/10.1085/jgp.201010495

The results show that mutating these residues greatly alters the effect of ATP on CLC-1. We have also constructed double mutants and have studied the effects of ATP and CTP or ATP and GTP on the wild-type (WT) and mutant channels. The results from ATP and CTP or ATP and GTP modulations of these channels suggest that the residue at position 634 very likely interacts directly with the base moiety of the nucleotide. Furthermore, individual mutations also show nonadditive effects on the ATP modulation of CLC-1, a sign for an energy coupling between these residues in interacting with the bound ATP molecule.

MATERIALS AND METHODS

Construction of the homology model of the C-terminal cytoplasmic domain of CLC-1

The sequence of human CLC-1 (Steinmeyer et al., 1991) from L598 to T874 was used to construct the homology model, corresponding to the sequence of CLC-5 from H578 to N737. Two segments in the CLC-1 C terminus, one from L598 to R672 (corresponding to H578 to I641 in CLC-5) and the other from P825 to T874 (corresponding to P687 to A736 of CLC-5), contain the sequence for the CBS1 and CBS2, respectively. However, the segment from residue 671 to residue 824 of CLC-1 is missing in CLC-5. It is unknown whether this segment is disordered (i.e., intrinsically unstructured) or not. Excluding this missing segment, the sequence alignment using Vector NTI software (Invitrogen) showed a sequence identity of 19.7% and a similarity of 31.3% between CLC-1 and CLC-5. Homology modeling was performed with a bound ATP molecule using the MODELLER program (Martí-Renom et al., 2000). The structures of the two segments containing the sequence of CBS domains of CLC-1 (Fig. 1, red and yellow) were determined using the crystal structure of CLC-5 as a template (Protein Data Bank accession no. 2J9L) with energy minimization using the MODELLER program. It can be seen that the missing segment between the two CBS domains (Fig. 1, dotted line) is remote from the bound ATP and thereby has little effect on the structures of the two CBS domains forming the ATP-binding site (Fig. 1).

Mutagenesis and channel expression

The ATP modulation of CLC-1 is controlled by oxidation and reduction (Zhang et al., 2008). We therefore chose *Xenopus laevis* oocytes as the channel expression system, and relatively large electrodes (with a tip diameter of ~7–10 µm) were used to excise large membrane patches because the ATP effect had previously been shown to be more stable using these experimental approaches compared with those using small patches excised from mammalian cells (Zhang et al., 2008). To further avoid decline of the current as a result of potential oxidation, all electrophysiological experiments were conducted in bath solutions containing 50–100 µM of reducing reagents (dithiothreitol or β-mercaptoethanol).

All mutants and the WT human CLC-1 Cl^- channel were constructed in the pTLN vector. Messenger RNAs were synthesized using the SP6 mMessage mMachine kit (Invitrogen). Harvesting *Xenopus* oocytes and the injection of messenger RNAs followed routine procedures as described previously (Chen, 1998; Li et al., 2005). Excised inside-out patch recordings were performed 3–5 d after RNA injections. The point mutants were constructed using the QuickChange II Site-Directed Mutagenesis kit (Agilent Technologies). The mutated region was confirmed by commercial DNA sequencing services.

Electrophysiological recordings

Electrophysiological experiments were conducted using the Axopatch 200B amplifier and the Digidata 1320 A/D board controlled by pClamp8 software (Axon Instruments/Molecular Devices). Signal digitization and filtering (by the digital filter in the pClamp8 program) were 10 kHz and 5 kHz, respectively. The tip diameter of the recording electrodes was relatively large, and these electrodes normally had a resistance of 0.4–0.6 MΩ when filled with a pipette (extracellular) solution containing 120 mM *N*-methyl-D-glucamine–Cl, 1 mM $MgCl_2$, 10 mM HEPES, and 1 mM EGTA, pH 7.4. Because the ATP effect was not prominent at a neutral pH_i, we examined the effect of ATP at pH_i 6.8. The bath (intracellular) solutions had the same ionic components, with pH_i being adjusted to 6.8 after the desired concentrations of ATP were added. Mg^{2+}-ATP was purchased from Sigma-Aldrich. A stock solution of 100 mM was made in distilled water and was stored at −20°C. Working solutions of ATP were made on the same day of the experiments.

For any given patch, the membrane potential of the excised patch was held at 0 mV. The voltage protocol used to construct

A

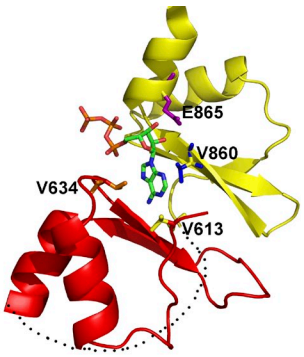

B

	V613	V634	V860 E865
	*	*	* *
CLC-1	RD---VKFVSA	LQTTTVKTLPL	GKLRGVLALEELQKAIE
CLC-0	RD---VTSIAS	LRQTKLKFFPF	GKLVGVVALAEIQAAIE
CLC-5	NDPLLTVLTQD	ISETTYSGFPV	GRLLGIITKKDVLKHIA
AtCLC-a	P-PVVTLN--G	LRNTTHNAFPV	SPVIGILTRQDLRAYNI

Figure 1. Homology modeling of the C-terminal domain of CLC-1. (A) Homology model of the CBS domain of CLC-1 shown in ribbon presentation. The two segments of CLC-1 sequence corresponding to CLC-5 are colored in red and yellow, whereas the segment that is missing in CLC-5 is illustrated with a dotted black line. ATP is shown in stick presentation (in CPK color). Key amino acids examined in this study are colored in yellow (V613), orange (V634), blue (V860), and purple (E865). (B) Sequence alignment of CLC-0, CLC-1, CLC-5, and AtCLC-a for the region encompassing the four residues shown in A.

the voltage dependence of the common gate open probability (P_o^c-V curve) has been described previously (Tseng et al., 2007; Zhang et al., 2008). This voltage protocol starts with a test voltage varying from 120 to −140 mV (in −20-mV steps) for 400 ms followed by a brief depolarizing voltage to 170 mV for 400 µs and then finally a tail voltage at −100 mV for 300 ms. Channel currents were recorded in a given patch both in the absence and in the presence of ATP. The current in response to the tail voltage was fitted to a double-exponential function, and the initial value of the tail current was determined by extrapolating the fitted curve to the start of the tail voltage. The initial tail current of each trace was then normalized to the initial tail current obtained after the 120-mV test voltage in the absence of ATP. Because the fast gate open probability is fully activated by the brief voltage step at 170 mV, the normalized initial tail current represents the open probability of the common gate (P_o^c) at the preceding test voltage (Accardi and Pusch, 2000; Duffield et al., 2003; Bennetts et al., 2005). The initial tail current in the presence of ATP was also normalized to the maximal tail current (with 120-mV test voltage) in the absence of ATP. The normalized value (or P_o^c) was then plotted against the test voltage, V. The half-activating voltage ($V_{1/2}$) of the P_o^c-V curve was determined by fitting the data points to a Boltzmann equation:

$$P_o^c = P_{min} + (1 - P_{min}) / \left\{1 + \exp\left[zF\left(V - V_{1/2}\right) / RT\right]\right\}.$$

The difference in $V_{1/2}$ (i.e., $\Delta V_{1/2}$) between the absence and presence of ATP was then determined as the qualitative response to a certain concentration of ATP.

Mutant cycle analyses

Data analyses and presentations were performed using the combination of pClamp8 and Origin software (Origin Laboratory). One way of evaluating the apparent affinity of ATP was to construct the dose-dependent curve by plotting $\Delta V_{1/2}$ as a function of the ATP concentration. The apparent $K_{1/2}$ value was then determined according to the Michaelis-Menten equation

$$\Delta V_{1/2} = \Delta V_{1/2,max} / \left(1 + K_{1/2} / [ATP]\right), \quad (1)$$

where $\Delta V_{1/2,max}$ is the maximal shift of the $V_{1/2}$ at saturated ATP concentrations, whereas $K_{1/2}$ is the apparent half-effective concentration in shifting the P_o^c-V curve. We used the aforementioned analysis for a qualitative comparison of the ATP effects. However, the apparent $K_{1/2}$ derived from the shift of $V_{1/2}$ does not truly reflect the half-point of ligand occupancy. To estimate the half-point of occupancy (or binding probability) of ATP, we used a four-state allosteric model to describe the opening and closing of the channel with or without ATP binding (Zifarelli and Pusch, 2009):

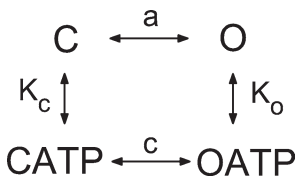

(SCHEME 1)

In Scheme I, C and O represent the closed and open states of the common gate, and *a* and *c* represent the gating equilibrium constants of the ATP-unbound and the ATP-bound channels. K_c and K_o are the binding dissociation constants of the closed-state and open-state channels for ATP, respectively. To determine K_o and K_c, the values of P_o^c at various ATP concentrations, namely P_o^c(ATP), were normalized to the P_o^c in the absence of ATP. The normalized values were then plotted against ATP concentrations (see Figs. 6 and 7) and were fit into Eq. 2 (Zifarelli and Pusch, 2009):

$$P_o^c(ATP) / P_o^c(control) = \left(1 + [ATP]/K_o\right) / \left(1 + [ATP]/K_c\right). \quad (2)$$

For mutant cycle analyses, the interaction between the ligand and the binding site can be altered by the perturbation on the ligand, the binding site, or both. The free energy of the interaction, which is determined from K_o or K_c ($\Delta G_o = RT\ln K_o$ and $\Delta G_c = RT\ln K_c$), can therefore be perturbed by manipulating the ligand and the receptor individually or simultaneously, thus forming a mutant cycle as shown in Fig. 6. If the two parts changed are independent of each other, the free energy perturbation caused by the double manipulation is equal to the sum of the free energy perturbations from individual manipulations. Namely,

$$\Delta G(X_2, Y_2) - \Delta G(X_1, Y_1) = [\Delta G(X_1, Y_2) - \Delta G(X_1, Y_1)] + [\Delta G(X_2, Y_1) - \Delta G(X_1, Y_1)], \quad (3)$$

where $\Delta G(X,Y)$ is the free energy of binding of the ligand Y to the channel X. A rearrangement of Eq. 3 leads to

$$\Delta G(X_1, Y_1) + \Delta G(X_2, Y_2) = \Delta G(X_1, Y_2) + \Delta G(X_2, Y_1)$$

or

$$RT\ln\left[K(X_1, Y_1) \times K(X_2, Y_2)\right] = RT\ln\left[K(X_1, Y_2) \times K(X_2, Y_1)\right],$$

where $K(X,Y)$ is K_o or K_c from the experiment in channel X using ligand Y. The coupling coefficient, Ω, for the two perturbations in this mutant cycle is defined as

$$\Omega = \left[K(X_1, Y_1) \times K(X_2, Y_2)\right] / \left[K(X_1, Y_2) \times K(X_2, Y_1)\right]. \quad (4)$$

When Ω is close to unity, there is little coupling energy between these two manipulations because the coupling energy of the pair of manipulations is given by $RT\ln\Omega \approx 0$. On the other hand, when Ω is significantly different from 1, the mutant cycle analysis suggests that the two manipulations are not independent. Previous studies have used mutant cycle analyses to identify the interacting residues located in the potassium channel pore and on the pore-blocking toxin, respectively (Hidalgo and MacKinnon, 1995; Naranjo and Miller, 1996; Ranganathan et al., 1996).

The mutant cycle approach can be modified for examining whether the free energy perturbations of two mutations within the binding site of ATP are additive. Examples are shown in Fig. 7. Again, an Ω value significantly deviating from unity suggests that these two mutations may be coupled energetically, and thus the two residues may interact with the bound ligand simultaneously.

Online supplemental material

Fig. S1 shows a comparison of the two homology models of CLC-1's C-terminal domain based on the high resolution structures of CLC-5 and CmCLC. Fig. S2 shows the values of Ω calculated from the P_o^c values at other voltages. Online supplemental material is available at http://www.jgp.org/cgi/content/full/jgp.201010495/DC1.

RESULTS

The C-terminal cytoplasmic regions of all eukaryote CLC molecules contain two tandem CBS domains that form a putative ATP-binding site (Scott et al., 2004;

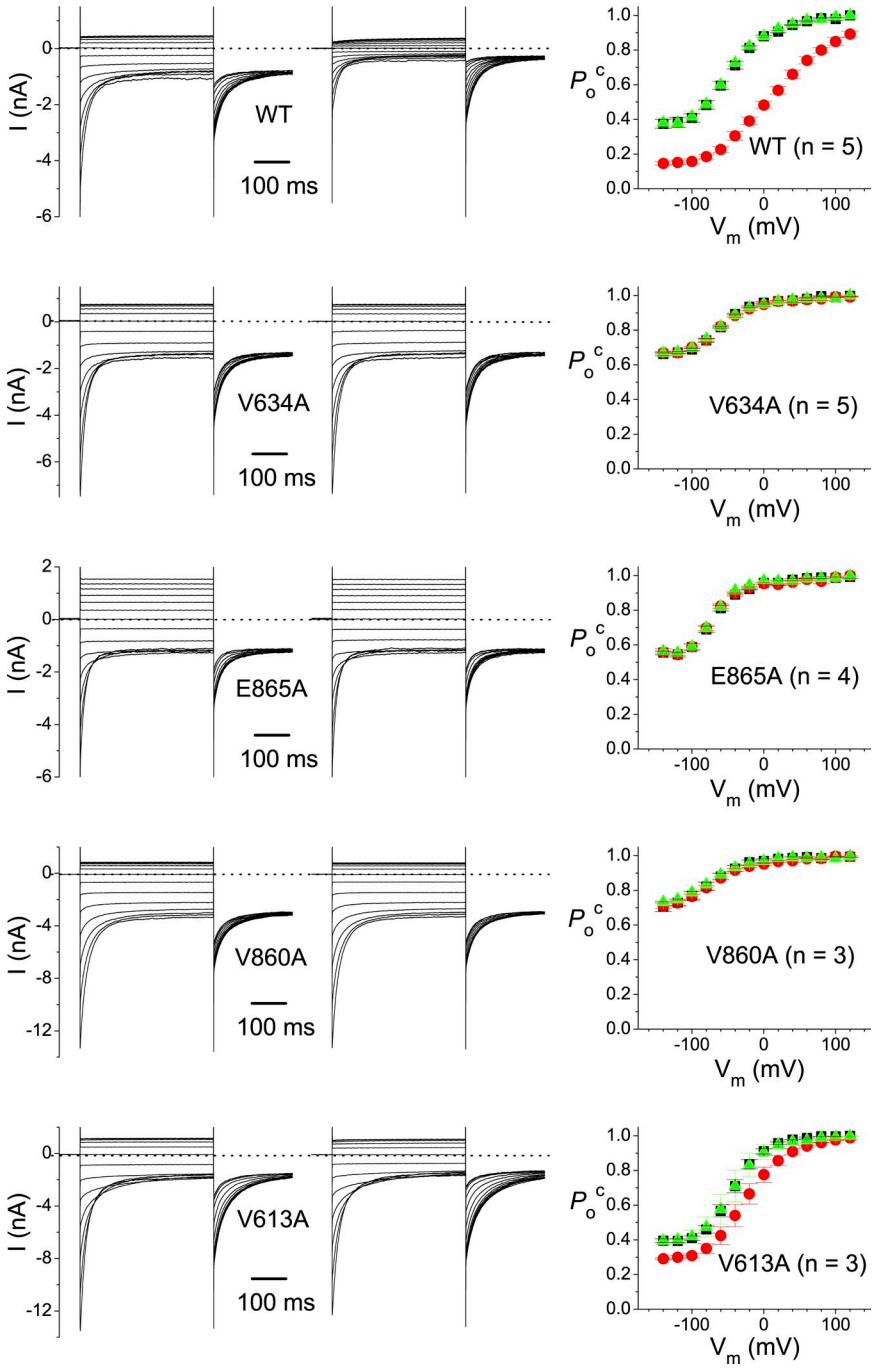

Figure 2. Effects of alanine mutations for four residues on the ATP modulation of CLC-1. (left and middle) Recording traces of WT CLC-1 and the four mutants. The recordings in the absence (left) and in the presence (middle) of 3 mM ATP were obtained from the same patch (pH_i 6.8). (right) Steady-state P_o^c-V curves of WT CLC-1 and the four alanine mutants shown in left and middle panels. Black squares, red circles, and green triangles represent the data in control (before ATP), 3 mM ATP, and washout, respectively.

Wellhauser et al., 2006). This predicted ATP-binding site has been directly observed in the high resolution structure of the C terminus of CLC-5 (Meyer et al., 2007). So far, functional consequences of ATP modulation have been shown in CLC-1 as well as in CLC-2, CLC-5, and AtCLC-a (Niemeyer et al., 2004; De Angeli et al., 2009; Zifarelli and Pusch, 2009). In this study, we use CLC-1 to study the interaction of ATP with CBS domains.

We first constructed a homology model of CLC-1's C-terminal region based on the high resolution, ATP-bound structure of the C-terminal domain of CLC-5 (Fig. 1 A). An independent model was built later based on the recently solved structure of CmCLC (Fig. S1 A). The homology model based on the CLC-5 structure suggested several residues that might interact with the bound ATP molecule, including V613, V634, V860, and E865. Other nearby residues, such as T636, P638, H847, and L848, appear to line the ATP-binding pocket as well. However, because the latter four residues in CLC-1 have been examined previously (see Fig. S1 B for the residues in CLC-1 whose mutations affect the ATP effect), we focused on the former four residues in this study. Fig. 1 B shows the alignment of the amino acid sequence from CLC-0, CLC-1, CLC-5, and AtCLC-a in

TABLE I

$V_{1/2}$ and P_{min} of the P_o^c-V curves of various mutants

Channels/mutants	$V_{1/2}$	P_{min}	*n*
WT CLC-1	−45.9 ± 2.8[a]	0.35 ± 0.02[a]	15
V634A	−59.3 ± 0.8	0.64 ± 0.02	7
V634D	−34.0 ± 3.9	0.28 ± 0.02	7
V634F	−56.8 ± 2.0	0.40 ± 0.01	9
V634Y	−72.4 ± 1.8	0.50 ± 0.02	7
V634C	−44.4 ± 2.5	0.30 ± 0.01	7
V634S	−58.3 ± 0.9	0.42 ± 0.02	4
V634G	−47.6 ± 2.8	0.32 ± 0.01	7
V634W	−54.7 ± 2.6	0.45 ± 0.02	4
E865A	−68.5 ± 2.6	0.52 ± 0.01	4
E865D	−36.2 ± 2.5	0.24 ± 0.01	11
E865S	−43.7 ± 8.2	0.32 ± 0.01	3
V860A	−74.6 ± 1.3	0.67 ± 0.02	3
V860S	−54.9 ± 7.6	0.26 ± 0.02	4
V860Y	−37.5 ± 8.1	0.28 ± 0.01	4
V613A	−49.1 ± 3.4	0.37 ± 0.01	7
V613F	−43.9 ± 8.7	0.28 ± 0.02	3
V613G	88.2 ± 4.7	0.15 ± 0.01	5

[a]Error from curve fitting.

regions containing the target residues. Among these four CLC molecules, functional ATP modulation effects have been observed in the latter three CLCs: ATP inhibits the activity of CLC-1 and AtCLC-a, whereas it potentiates the activity of CLC-5. The homology model suggested that the adenine ring of ATP appears to be surrounded by the side chains of V634, V860, and V613, whereas E865 may interact with the ribose of ATP. Among these four positions, two corresponding residues in CLC-5 were examined previously by others (Meyer et al., 2007; Zifarelli and Pusch, 2009). The ATP binding was shown to be eliminated by the Y617A and D727A mutations of CLC-5 (corresponding to V634A and E865A of CLC-1). Mutating two equivalent residues, H620 and D753 (corresponding to V634 and E865 of CLC-1), also diminished the ATP inhibitory effect in AtCLC-a (De Angeli et al., 2009). In addition, T596 and I722 of CLC-5 (corresponding to V613 and V860 of CLC-1) have also been suggested to be involved in ATP binding to CLC-5 (Meyer et al., 2007). Thus, V613, V634, V860, and E865 of CLC-1 are likely to interact with the bound ATP molecule.

We started our experiments by examining the ATP modulation effects on the mutants in which the WT residues at these four positions were replaced by alanine. Fig. 2 shows the effects of ATP on WT CLC-1 and those of the four alanine mutants at pH_i 6.8. The recording traces were elicited by the voltage protocol used for constructing the common gate P_o^c-V curve (see Materials and methods). The comparison of the recording traces both in the absence (Fig. 2, left) and in the presence of 3 mM ATP (Fig. 2, middle) shows a robust inhibition of WT CLC-1 by ATP (Fig. 2, top), but the effect of ATP on these alanine mutants is either weak or completely lost. The P_o^c-V curves shown in Fig. 2 (right) indicate that the V634A, V860A, or E865A mutation eliminates the ATP modulation effect and the V613 mutation significantly reduces the ATP effect.

As an initial effort to explore the interaction of ATP with the potential binding site more systemically, we replaced the WT residues with multiple amino acids at

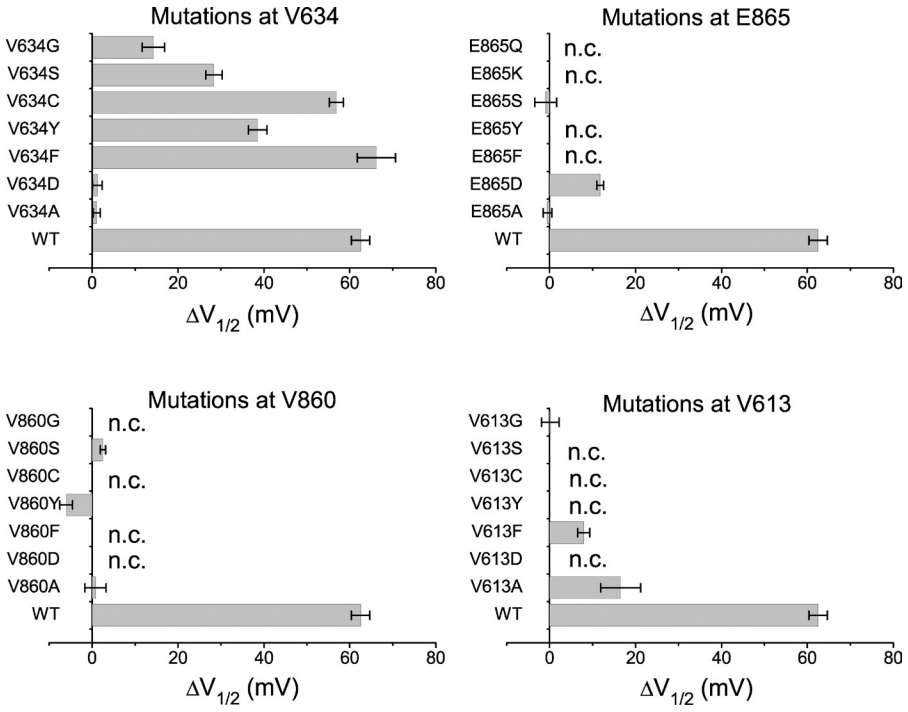

Figure 3. Changes of the $V_{1/2}$ of the P_o^c-V curves of various mutants in response to 3 mM ATP at pH_i 6.8. The P_o^c-V curves of each mutant in the absence and in the presence of 3 mM ATP were constructed from the same patch, and the $V_{1/2}$ of the P_o^c-V curves were obtained by fitting the data points to a Boltzmann equation. The difference in $V_{1/2}$ between control and 3 mM ATP ($\Delta V_{1/2}$) was first determined from each patch and then averaged (n = 14 for WT CLC-1 and n = 4–7 for various mutants). The label n.c. indicates that the mutant did not show functional current in at least two runs of expression in *Xenopus* oocytes. Error bars represent SEM.

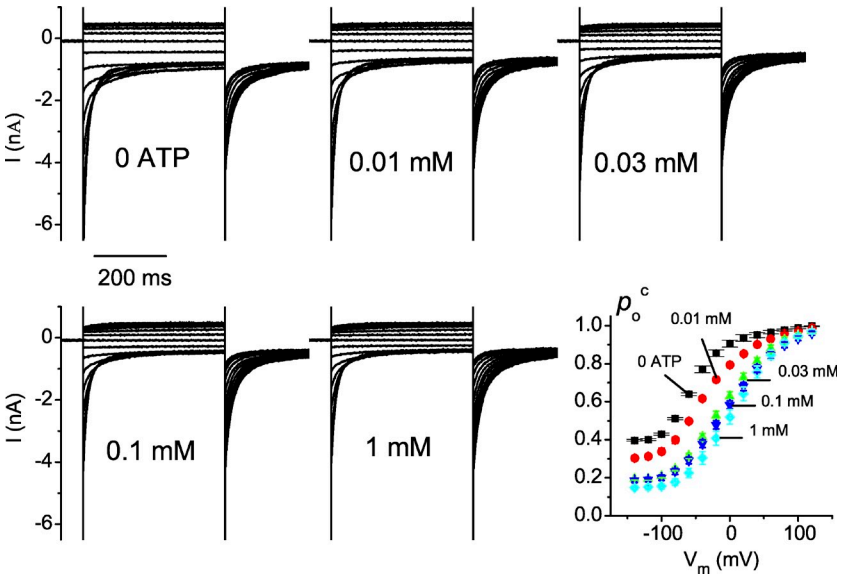

Figure 4. The V634F mutation increases the apparent affinity for the ATP modulation. Representative recording traces were obtained from an excised patch of the oocyte expressing the V634F mutant in control (0 ATP) and in various concentrations of ATP as indicated. The averaged P_o^c-V curves of the V634F mutant in various ATP concentrations are shown in the bottom right panel. Error bars represent SEM. $n = 7$.

these four positions. Mutating V613, V860, and E865 affects the functional expression; at each site, four out of seven mutants did not generate functional current in *Xenopus* oocytes. However, mutations at the V634 position are more tolerable; all mutants made in this study at this position showed functional current. Table I summarizes the minimal open probability (P_{min}) and the half-activation voltage ($V_{1/2}$) of the common gate P_o^c-V curve of these functional mutants. We then tested the shift of the P_o^c-V curve in the functional mutants by 3 mM ATP at pH_i 6.8. Fig. 3 shows the change of the $V_{1/2}$ ($\Delta V_{1/2}$) of the P_o^c-V curve in response to 3 mM of intracellular ATP (pH_i 6.8). For mutations at positions V613, V860, and E865, all functional mutants show a substantial reduction of $\Delta V_{1/2}$ in response to 3 mM ATP. However, the effects of mutations at the V634 position are diverse. The V634A, V634D, V634G, and V634S mutations suppress the ATP effects, whereas the ATP modulation of V634C is similar to that of the WT channel. Interestingly, some mutants, for example V634F, show a higher sensitivity to the ATP modulation. Although the $\Delta V_{1/2}$ of V634F generated by 3 mM ATP appears to be similar to that of WT CLC-1 (Fig. 3), the apparent affinity of ATP in shifting the P_o^c-V curve of this mutant is higher than that of WT CLC-1—the shift nearly reached a maximum at a concentration of 0.1 mM (Fig. 4).

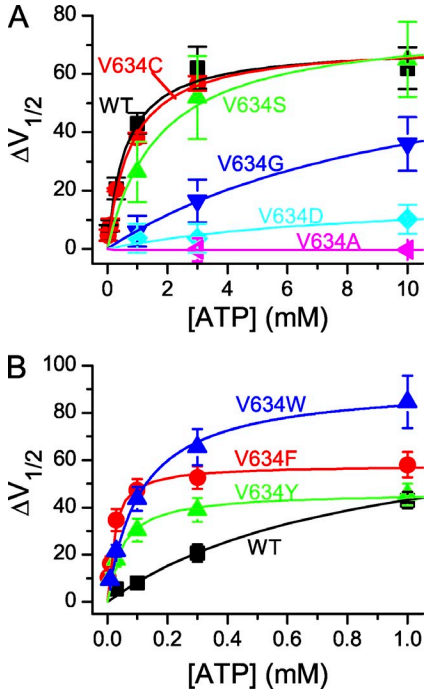

Figure 5. Shift of the $V_{1/2}$ of the P_o^c-V curve ($\Delta V_{1/2}$) in various mutants of V634 as a function of the ATP concentration. Data points were fitted to Eq. 1 to determine the apparent $K_{1/2}$ and $V_{1/2,max}$. (A) Mutants of V634 in which the apparent ATP affinity is reduced. For comparison, the ATP dose–response curve of WT CLC-1 is also shown. (B) ATP dose-dependent curves of WT CLC-1, V634F, V634Y, and V634W. Error bars represent SEM. $n = 4$–8.

To examine the diverse functional consequences of mutating residue V634, we studied the ATP dose-dependent effect in various V634 mutants. Fig. 5 A shows the dose–response curves of those mutants with less ATP sensitivity, whereas Fig. 5 B depicts the results of mutants with a higher ATP sensitivity. The $K_{1/2}$ and the maximal value of the $V_{1/2}$ shift ($\Delta V_{1/2,\,max}$) are shown in Table II. The ATP modulations of V634C and V634S mutants are roughly similar to that of the WT channel: the $\Delta V_{1/2,\,max}$ in both cases is similar to that of the WT channel, whereas the apparent affinity is only slightly reduced in the V634S mutant. However, the V634D and V634G mutants show a more severe disruption in ATP regulation: the apparent ATP affinity and/or the maximal shift of the $V_{1/2}$ is reduced in these two mutants. Finally, the V634A mutation completely eliminates the ATP modulation effect; even at an ATP concentration of 10 mM, no significant shift of $V_{1/2}$ is observed. However, placing

TABLE II

$K_{1/2}$ and $\Delta V_{1/2,max}$ for the ATP dose–response curves of V634 mutants

Channels/mutants	$K_{1/2}$	$\Delta V_{1/2,\ max}$	*n*
	mM	*mV*	
WT CLC-1	0.78 ± 0.08	76.9 ± 7.4	8
V634F	0.026 ± 0.002	61.6 ± 4.9	7
V634Y	0.050 ± 0.004	46.6 ± 3.3	5
V634W	0.11 ± 0.01	90.7 ± 9.4	4
V634C	0.81 ± 0.06	70.8 ± 3.3	5
V634S	1.8 ± 0.3	72.9 ± 8.5	4
V634D	7.4 ± 1.5	18.5 ± 3.1	4
V634G	13.3 ± 4.0	77.8 ± 8.1	4
E865D	0.40 ± 0.09	14.2 ± 2.4	6
V613A	2.3 ± 0.3	26.3 ± 3.4	4
E865D-V634F	0.089 ± 0.05	8.7 ± 2.4	4
V613A-V634F	2.3 ± 0.35	62.6 ± 5.4	7

$K_{1/2}$ determined from Eq. 1, using $\Delta V_{1/2}$ as the response to ATP inhibition. Means ± SEM are given.

aromatic amino acids at position 634 appears to enhance the ATP modulation. The apparent $K_{1/2}$ of the ATP effects are 0.026, 0.050, and 0.11 mM for V634F, V634Y, and V634W (Table II), corresponding to an increase of the apparent ATP affinity by ∼30-, ∼16-, and ∼7-fold, respectively.

Because only those mutants with an aromatic side chain at the V634 position showed a high ATP sensitivity (namely V634F, V634Y, and V634W), we suspected that the ring–ring interaction may contribute to the higher apparent ATP affinity in these mutants. If the adenine of ATP indeed directly interacts with the side chain of residue at position 634, we expect that a mutant cycle analysis should reveal that the free energy perturbations caused by mutating residue 634 and by altering the base of the nucleotide should couple energetically.

However, the estimate of the apparent affinity of ATP inhibition based on the change of $V_{1/2}$ could be problematic because $\Delta V_{1/2}$ may not truly reflect the change of ligand occupancy. For this reason, we model the ATP inhibitory effect using a four-state allosteric scheme (Scheme I) to evaluate the affinities of WT CLC-1 and V634F mutants for ATP and other nucleotides. Fig. 6 gives an example of mutant cycle analysis in which the normalized P_o^c at −40 mV in different conditions are plotted against ligand concentrations. Fig. 6 A shows that the free energy changes caused by individual perturbations are not additive, with large Ω values (see Materials and methods) of 60 and 113 calculated from the values of K_c and K_o, respectively. We have also performed similar analysis for WT CLC-1 and V634F using ATP and GTP as ligands (Table III), with a calculated Ω of ∼7.6–10. However, when deoxy-ATP (dATP) was used to examine the interaction of the base with the side chain of residue 634, Ω values close to 1 were obtained (Fig. 6 B and Table III). Analyses of P_o^c at various voltages revealed similar Ω values in the voltage range between −140 and −40 mV (Fig. S2 A). These results again are consistent with the idea that the base of the bound nucleotide directly interacts with the side chain of residue 634 of CLC-1.

The homology model of CLC-1 also suggests that V613, V860, and E865 may interact with ATP. We thus examined the perturbations of the binding free energy of ATP to see whether these changes induced by individual mutations are additive. Unfortunately, construction of the ATP dose-dependent curve for V860 mutants is difficult because of the very small shift of the P_o-V curve caused by ATP. We therefore focused on V613 and E865 and studied the synergistic effects between V634F and V613A and between V634F and E865D mutations because these mutations still retain some degree of ATP inhibition and at the same time alter the apparent ATP affinity. The concentration-dependent curves of the ATP-induced change of P_o^c for the single and double mutants were constructed, and the ATP affinity (K_o and K_c of Scheme I) for each mutant was compared with that of WT CLC-1. Fig. 7 A shows a double mutant cycle analysis that examines the interaction of the V634F and V613A mutations, whereas Fig. 7 B shows the analysis of the interaction between V634F and E865D.

TABLE III

Apparent affinities of ATP, CTP, GTP, and dATP for WT CLC-1 and V634F

Channels/mutants	K_o or K_c			
	ATP	CTP	GTP	dATP
	mM	*mM*	*mM*	*mM*
K_c				
WT CLC-1	0.32 ± 0.04 (8)	1.1. ± 0.2 (6)	9.9 ± 1.0 (5)	0.85 ± 0.14 (4)
V634F	0.017 ± 0.005 (7)	3.5 ± 0.4 (8)	4.0 ± 0.6 (6)	0.049 ± 0.013 (6)
		Ω = 60	Ω = 7.6	Ω = 1.09
K_o				
WT CLC-1	0.70 ± 0.10 (8)	1.3. ± 0.3 (6)	15.1 ± 1.9 (5)	1.3 ± 0.2 (4)
V634F	0.039 ± 0.013 (7)	8.2 ± 1.2 (8)	8.5 ± 1.6 (6)	0.071 ± 0.021 (6)
		Ω = 113	Ω = 10	Ω = 0.98

Calculated from the values of P_o^c at −40 mV. Means ± SEM are given. The numbers inside parentheses indicate the number of patches.

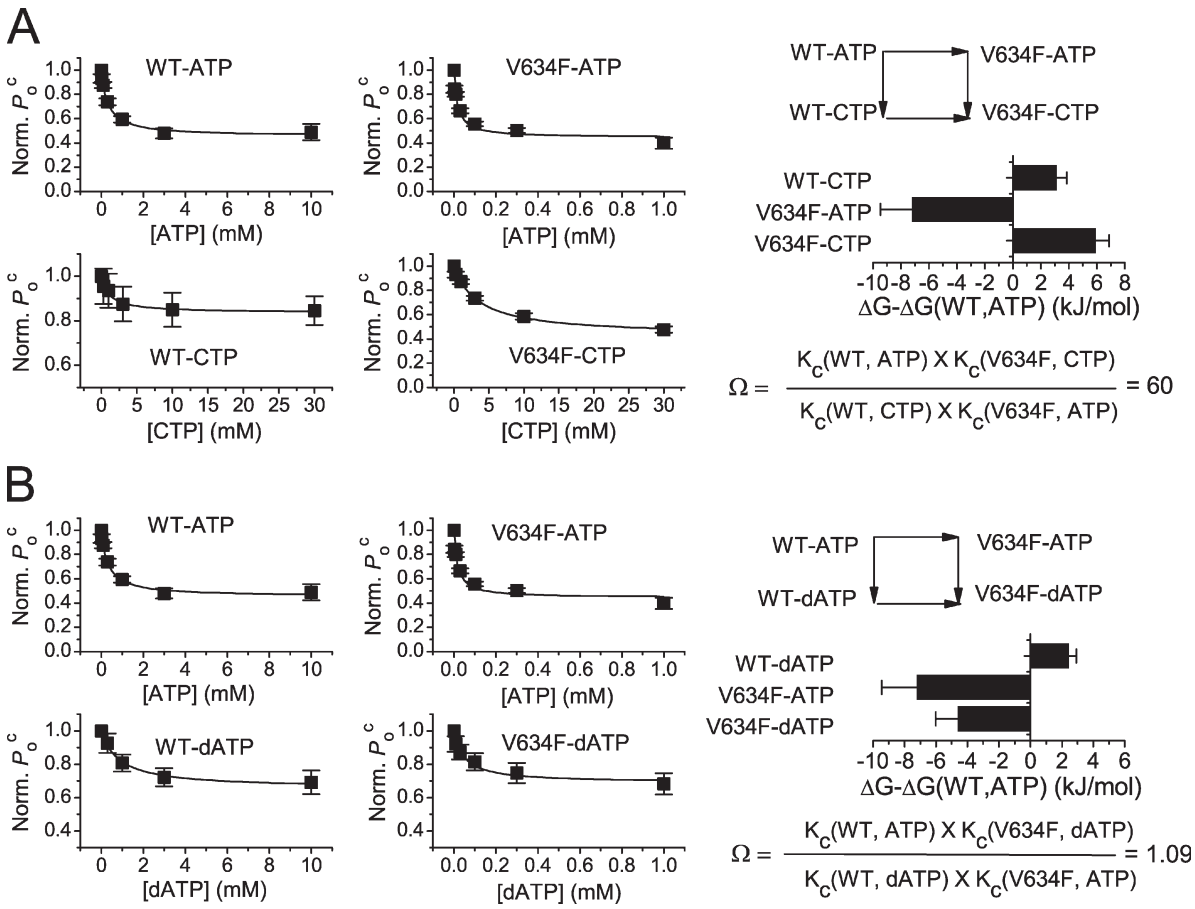

Figure 6. Interaction of nucleotides with residue V634 in the ATP-binding site explored by double mutant cycle analyses. (A) Mutant cycle analysis of the interaction of the nucleotide with residue V634. The ATP and CTP dose–response curves of WT CLC-1 and the V634F mutant were first constructed using the parameter P_o^c(ATP)/P_o^c(control) as the dependent parameter. The values of K_o and K_c (Table III) of ATP/CTP modulations were determined by fitting the data points to Eq. 2, and the K_c values were used to calculate the free energy differences of single or double manipulations (bar graph) according to Eq. 3 and the coupling constant, Ω, according to Eq. 4. n = 6–8. (B) Mutant cycle analysis of the nucleotide interaction with V634 using ATP and dATP. The ligand dose–response curves of WT CLC-1 and V634F were constructed using P_o^c(ATP)/P_o^c(control) as the dependent parameter. K_o and K_c were determined (Table III), and the Ω value and the free energy differences were calculated accordingly. n = 4–8.

Although the value of Ω for the former pair of mutations appears to be large, whereas that of the latter pair of mutations is smaller (see Fig. S2 B for Ω values at different voltages), the results in both cases suggest that the mutational effects of V634F and those of V613A and E865D on the ATP regulation may couple together, a result consistent with the idea that these residues interact with ATP simultaneously.

DISCUSSION

CLC-1 Cl^- channels contribute a major conductance to the sarcolemmal membrane of skeletal muscles and, thus, are critical for the membrane excitability of skeletal muscles. The importance of CLC-1 in maintaining normal muscle functions can be seen from the myotonia disease resulting from defects of CLC-1 (Koch et al., 1992). Likely, the CLC-1 conductance facilitates repolarization of the membrane of skeletal muscles after firing an action potential (Jentsch et al., 2005). In addition, recent studies suggested that the reduction of the Cl conductance of the sarcolemma by a low intracellular pH (pH_i) can help overcome muscle fatigue (Pedersen et al., 2004, 2005). Experiments performed several decades ago showed that acidification of muscle cells can reduce the muscle Cl conductance (Hutter and Warner, 1967a,b). However, various experiments on the cloned CLC-1 channel showed that reducing pH_i increases the open probability of CLC-1 (Rychkov et al., 1996; Saviane et al., 1999; Accardi and Pusch, 2000). On the other hand, we and others recently found that if ATP is included in the intracellular solution, reducing pH_i decreases the CLC-1 activity (Bennetts et al., 2007; Tseng et al., 2007). Thus, binding of ATP to the intracellular side of CLC-1 appears to be a prerequisite for reducing the CLC-1 conductance by a low pH_i.

The primary sequences of CLC channels/transporters have suggested the presence of a potential ATP-binding

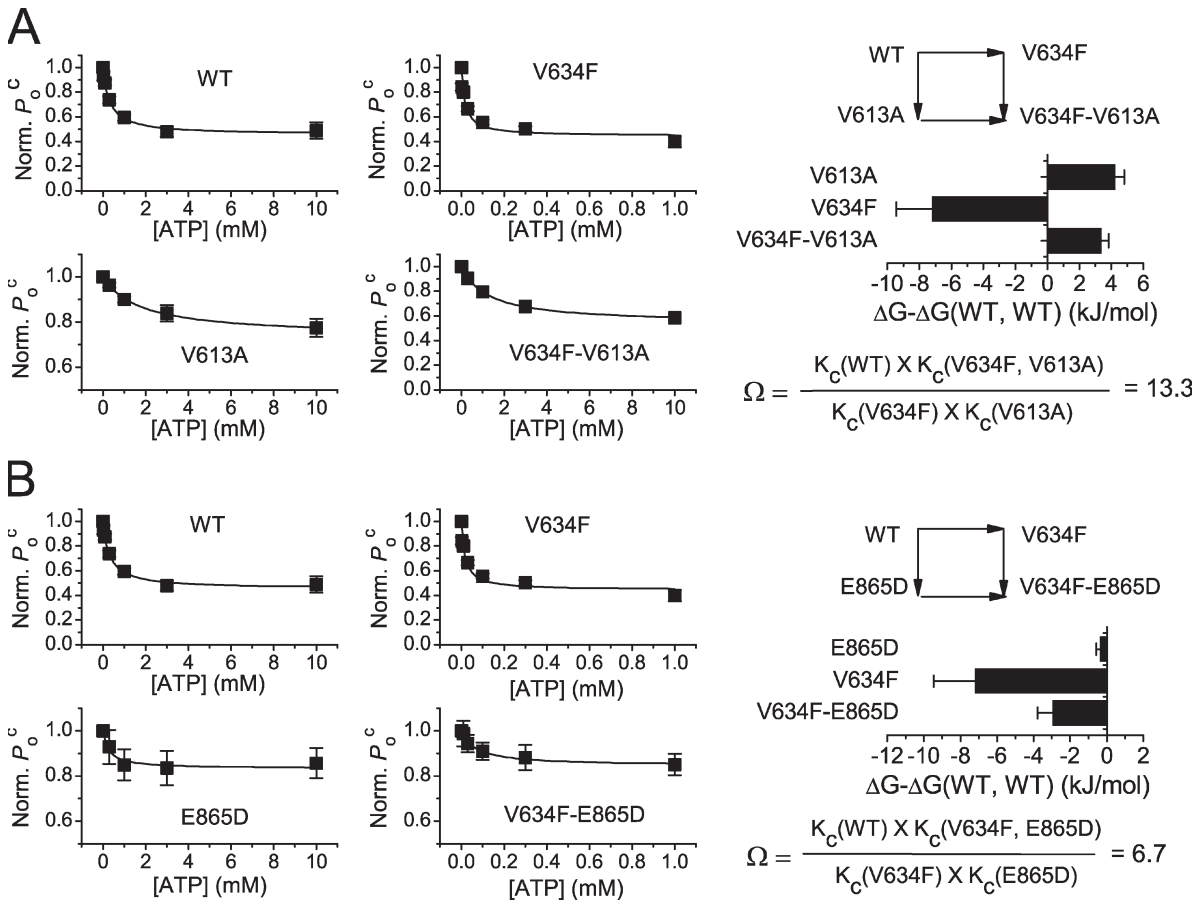

Figure 7. Nonadditive effects of mutations on the ATP modulations of CLC-1. The parameter $P_o^c(\text{ATP})/P_o^c(\text{control})$ was used as the response to ATP modulation. (A) Mutant cycle analysis of the effects of V634F and V613A mutations on the ATP modulation. ATP dose–response curves of single point mutants and the double mutants were constructed to determine the values of K_o and K_c. The fitted K_c values were used to calculate the free energy differences of single or double mutants (bar graph) according to Eq. 3 and the coupling constant, Ω, according to Eq. 4. In the context of Eq. 2, the V634F mutation corresponds to the change from X_1 to X_2, whereas the V613A mutation represents the change from Y_1 to Y_2. (B) Double mutant cycle analysis for V634F/E865D mutations. The values of Ω at different voltages are shown in Fig. S2. Error bars represent SEM. $n = 4–8$.

site in the CBS domain located at the C terminus of CLC molecules. Structural and biochemical experiments on the C-terminal domain of CLC-5 demonstrated that ATP indeed binds to the predicted CBS domain of CLC-5 (Meyer et al., 2007). Does ATP also bind to the CBS domain of CLC-1 and cause the inhibition of the CLC-1 current? Recent studies from different laboratories provided somewhat inconsistent results. Our results (Tseng et al., 2007) and those from Bennetts et al. (2007) showed that ATP may modulate the common gating of CLC-1. On the other hand, Zifarelli and Pusch (2008) failed to show an ATP effect on CLC-1 and thus suggested that the ATP modulation of CLC-1 may be achieved via an accessory protein. Although our further experiments showed that the ATP regulation of CLC-1 is modulated by oxidation and reduction (Zhang et al., 2008) and thus suggested that the variation of the oxidation reduction level in various experimental conditions could be one of the underlying reasons for inconsistent experimental findings, the evidence of a direct ATP binding to CLC-1 has still been lacking. With the studies outlined here, we have directly examined the interaction of ATP with the amino acid residues lining the potential ATP-binding pocket in the CBS domains of CLC-1.

To identify the potential residues in CLC-1 that may interact with the ATP molecule, we constructed homology models of CLC-1 based on the C-terminal structures of CLC-5 and CmCLC. Previously, two homology models have been reported for the C-terminal domain of CLC-1. One of them (Bennetts et al., 2005) was constructed based on the crystal structure of inosine-monophosphate dehydrogenase (Zhang et al., 1999), which is not very reliable because of the low sequence identity between CLC-1 and inosine-monophosphate dehydrogenase (Bennetts et al., 2007). The other model rebuilt by Bennetts et al. (2007) was based on the crystal structure of the C-terminal domain of CLC-0 (Protein Data Bank accession no. 2D4Z), which is an apo structure with no bound ATP molecule. The alignment between

the C-terminal structures of CLC-0 and CLC-5 shows a somewhat different orientation of the two CBS domains (Meyer et al., 2007). Similarly, the two CLC-1 C-terminal models we built based on CLC-5 and CmCLC structures also show quite a significant difference in the relative positions of the two CBS domains (and thus the residues interacting with ATP; Fig. S1). It cannot be excluded at this moment that part of the difference among various C-terminal structures results from an ATP-induced conformational change. Because the structure of the CLC-5's C-terminal domain contains ATP, we used the homology model based on this structure to guide our experiments.

Although CLC-1 and CLC-5 only show ~20% sequence identity, the homology model of the potential ATP-binding site in CLC-1 is quite similar to that in the C-terminal structure of CLC-5. For example, the residues V634 and E865 that correspond to Y617 and D727 of CLC-5 in sequence alignment are also located in the ATP-binding sites, and their side chains appear to interact with the adenine ring and the ribose of the bound ATP, respectively (Fig. 1), just like in the structure of the CLC-5 C-terminal domain. Mutating both V634 and E865 into alanine eliminates the ATP effect, a result consistent with biochemical data from CLC-5. In addition, the homology model also suggests that two other residues, V613 and V860, may also interact with ATP. Mutating these four residues in the potential ATP-binding pocket resulted in various consequences. Overall, the mutations at the V634 position are relatively tolerable for the functional expression of the channel. All mutations here resulted in functional mutant channels. For the mutations at positions V613, V860, and E865, four out of seven mutations at each position did not produce functional current. We have not characterized whether the mutations at these three positions resulted in nonfunctional channels or whether the mutations simply caused a problem of membrane trafficking. For those mutants that can generate functional current, the ATP regulation of CLC-1 was altered.

Overall, the majority of the mutants cause a suppression of the ATP effect; either the apparent affinity ($K_{1/2}$) or the efficacy (the maximal $\Delta V_{1/2}$) of the ATP modulation is reduced, or both. However, introducing an aromatic residue at position 634 generates mutant channels with a higher apparent ATP affinity. It is worth pointing out that WT CLC-1 contains a valine residue at position 634, whereas the corresponding residue in CLC-5 is tyrosine. The apparent $K_{1/2}$ of the ATP in WT CLC-1 at pH_i 6.8 is higher than that in CLC-5 (~90 µM) observed by Meyer et al. (2007) based on a binding assay, although a patch-clamp study by Zifarelli and Pusch (2009) reported that the ATP affinities of CLC-5 are 0.43 mM and 0.89 mM for the active and inactive states of this transporter, respectively. Nonetheless, both studies showed that the corresponding residue (Y617) in CLC-5 is crucial for the ATP modulation. Because placing aromatic amino acids at position 634 increased the apparent ATP affinity, we hypothesized that the aromatic ring of these amino acids may directly interact with the adenine of ATP. To further explore this possibility, we studied the apparent affinities of various nucleotides on WT CLC-1 and on the V634F mutant and showed that the Ω values from mutant cycle analyses are significantly deviated from unity for ATP/CTP and ATP/GTP pairs (Fig. 6 A and Table III). However, using ligands that differ in the ribose moiety (dATP vs. ATP) as the modulation ligands showed that the Ω value is close to unity (Fig. 6 B and Table III). These results are consistent with the hypothesis that the base moiety of the bound nucleotide in the CBS domain of CLC-1 interacts directly with residue V634.

Thus, the amino acid residue of V634 in CLC-1, like the corresponding residue in CLC-5 (Y617), should be critical for ATP binding to the CBS domain. In addition to V634, three other amino acid residues shown in this study also affect the ATP modulation of CLC-1. We wondered whether the mutations at these various positions affect the ATP binding independently. If so, the free energy change generated by the double mutation is expected to be a summation of the free energy changes from individual mutations. For this purpose, we used mutant cycle analyses to examine the interaction between the mutation V634F and two other mutations, V613A and E865D. We chose these two latter mutations because the mutants still retain some ATP inhibitions for constructing a reliable ATP dose-dependent curve. The apparent $K_{1/2}$ of the ATP modulations for the single point mutants and the double mutants are shown in Table II. Fig. 7 A shows the double mutant cycle analysis for V613A and V634F mutations. The results show a violation of the independency of the two mutations because the Ω value from this mutant cycle analysis clearly deviates from unity, indicating that the free energy change of the double mutant V613A/V634F (compared with the WT channel) is not the sum of the free energy changes from the V613A and V634F mutations. In comparison, experiments with V634F and E865D mutants appear to have a smaller Ω value of only ~6.7 (Fig. 7 B). We have no definitive interpretation of the large coupling energy between V613A and V634F mutations and the small coupling energy between V634F and E865D except speculating that V613 and V634 interact with the adenine ring of ATP, whereas V634 and E865 may be separated in farther distance. Nonetheless, the nonadditive effects of individual mutations and the strong energetic coupling in ATP/CTP and ATP/GTP bindings provide evidence against the idea that the ATP modulation on CLC-1 is mediated by an accessory protein.

Previous studies by others and our own experiments showed that the inhibition of the CLC-1 common gating by ATP can also be achieved by ADP and AMP

(Bennetts et al., 2005; Zhang et al., 2008). It was shown that there is no discrimination in binding ATP, ADP, and AMP to the CBS domains of CLC-5 (Meyer et al., 2007). This similarity seems to argue for a similar overall architecture of the two binding sites, although the sequence homology of the CBS domains of CLC-1 and CLC-5 is quite low (~30%). However, binding of nucleotides/nucleosides to CLC-5 potentiates but does not inhibit the transport activity of CLC-5 (Zifarelli and Pusch, 2009). In AtCLC-a, however, it was found that ATP has an inhibitory effect, whereas ADP and AMP do not have any direct effect except that AMP is able to compete with ATP for binding (De Angeli et al., 2009). The molecular basis underlying these detailed functional variations among the nucleotide/nucleoside effects of these three CLC molecules remains unclear. One possible explanation is that binding of nucleotides/nucleosides to the CBS domain may induce different allosteric effects in different CLC molecules. Thus, the ATP modulation mechanisms could be quite different in various CLC molecules (Zifarelli and Pusch, 2009).

In summary, the experiments presented in this study have identified several amino acid residues that may directly interact with the bound ATP molecule in the CBS domain of CLC-1. The results thus argue that ATP modulates the common gating of CLC-1 via a direct binding to the C-terminal domain of CLC-1. Given the large shift of the P_o^c-V curve, modulation of the CLC-1 common gating should be a useful model to study ATP interaction with the CBS domain. It will also be interesting to examine the functional roles of the corresponding residues in other CBS domain–containing molecules. Such a comparison of the effects of the corresponding mutations in different molecules could provide a deeper understanding of the molecular interaction between nucleotide and the CBS domain.

We thank Dr. Robert Fairclough for critical readings of the manuscript.

This study is supported by a National Institutes of Health grant (R01GM065447) to T.-Y. Chen. X. Zou is partially supported by a National Institutes of Health grant (R21GM088517).

Christopher Miller served as editor.

Submitted: 28 June 2010
Accepted: 9 March 2011

REFERENCES

Accardi, A., and M. Pusch. 2000. Fast and slow gating relaxations in the muscle chloride channel CLC-1. *J. Gen. Physiol.* 116:433–444. doi:10.1085/jgp.116.3.433

Bennetts, B., G.Y. Rychkov, H.L. Ng, C.J. Morton, D. Stapleton, M.W. Parker, and B.A. Cromer. 2005. Cytoplasmic ATP-sensing domains regulate gating of skeletal muscle ClC-1 chloride channels. *J. Biol. Chem.* 280:32452–32458. doi:10.1074/jbc.M502890200

Bennetts, B., M.W. Parker, and B.A. Cromer. 2007. Inhibition of skeletal muscle ClC-1 chloride channels by low intracellular pH and ATP. *J. Biol. Chem.* 282:32780–32791. doi:10.1074/jbc.M703259200

Chen, T.Y. 1998. Extracellular zinc ion inhibits ClC-0 chloride channels by facilitating slow gating. *J. Gen. Physiol.* 112:715–726. doi:10.1085/jgp.112.6.715

Chen, T.Y. 2005. Structure and function of clc channels. *Annu. Rev. Physiol.* 67:809–839. doi:10.1146/annurev.physiol.67.032003.153012

De Angeli, A., O. Moran, S. Wege, S. Filleur, G. Ephritikhine, S. Thomine, H. Barbier-Brygoo, and F. Gambale. 2009. ATP binding to the C terminus of the *Arabidopsis thaliana* nitrate/proton antiporter, AtCLCa, regulates nitrate transport into plant vacuoles. *J. Biol. Chem.* 284:26526–26532. doi:10.1074/jbc.M109.005132

Duffield, M., G. Rychkov, A. Bretag, and M. Roberts. 2003. Involvement of helices at the dimer interface in ClC-1 common gating. *J. Gen. Physiol.* 121:149–161. doi:10.1085/jgp.20028741

Feng, L., E.B. Campbell, Y. Hsiung, and R. MacKinnon. 2010. Structure of a eukaryotic CLC transporter defines an intermediate state in the transport cycle. *Science.* 330:635–641. doi:10.1126/science.1195230

Hidalgo, P., and R. MacKinnon. 1995. Revealing the architecture of a K+ channel pore through mutant cycles with a peptide inhibitor. *Science.* 268:307–310. doi:10.1126/science.7716527

Hutter, O.F., and A.E. Warner. 1967a. The effect of pH on the 36-Cl efflux from frog skeletal muscle. *J. Physiol.* 189:427–443.

Hutter, O.F., and A.E. Warner. 1967b. The pH sensitivity of the chloride conductance of frog skeletal muscle. *J. Physiol.* 189:403–425.

Jentsch, T.J., V. Stein, F. Weinreich, and A.A. Zdebik. 2002. Molecular structure and physiological function of chloride channels. *Physiol. Rev.* 82:503–568.

Jentsch, T.J., M. Poët, J.C. Fuhrmann, and A.A. Zdebik. 2005. Physiological functions of CLC Cl- channels gleaned from human genetic disease and mouse models. *Annu. Rev. Physiol.* 67:779–807. doi:10.1146/annurev.physiol.67.032003.153245

Koch, M.C., K. Steinmeyer, C. Lorenz, K. Ricker, F. Wolf, M. Otto, B. Zoll, F. Lehmann-Horn, K.H. Grzeschik, and T.J. Jentsch. 1992. The skeletal muscle chloride channel in dominant and recessive human myotonia. *Science.* 257:797–800. doi:10.1126/science.1379744

Li, Y., W.P. Yu, C.W. Lin, and T.Y. Chen. 2005. Oxidation and reduction control of the inactivation gating of Torpedo ClC-0 chloride channels. *Biophys. J.* 88:3936–3945. doi:10.1529/biophysj.104.055012

Markovic, S., and R. Dutzler. 2007. The structure of the cytoplasmic domain of the chloride channel ClC-Ka reveals a conserved interaction interface. *Structure.* 15:715–725. doi:10.1016/j.str.2007.04.013

Martí-Renom, M.A., A.C. Stuart, A. Fiser, R. Sánchez, F. Melo, and A. Sali. 2000. Comparative protein structure modeling of genes and genomes. *Annu. Rev. Biophys. Biomol. Struct.* 29:291–325. doi:10.1146/annurev.biophys.29.1.291

Meyer, S., and R. Dutzler. 2006. Crystal structure of the cytoplasmic domain of the chloride channel ClC-0. *Structure.* 14:299–307. doi:10.1016/j.str.2005.10.008

Meyer, S., S. Savaresi, I.C. Forster, and R. Dutzler. 2007. Nucleotide recognition by the cytoplasmic domain of the human chloride transporter ClC-5. *Nat. Struct. Mol. Biol.* 14:60–67. doi:10.1038/nsmb1188

Naranjo, D., and C. Miller. 1996. A strongly interacting pair of residues on the contact surface of charybdotoxin and a Shaker K+ channel. *Neuron.* 16:123–130. doi:10.1016/S0896-6273(00)80029-X

Niemeyer, M.I., Y.R. Yusef, I. Cornejo, C.A. Flores, F.V. Sepúlveda, and L.P. Cid. 2004. Functional evaluation of human ClC-2 chloride channel mutations associated with idiopathic generalized epilepsies. *Physiol. Genomics.* 19:74–83. doi:10.1152/physiolgenomics.00070.2004

Pedersen, T.H., O.B. Nielsen, G.D. Lamb, and D.G. Stephenson. 2004. Intracellular acidosis enhances the excitability of working muscle. *Science.* 305:1144–1147. doi:10.1126/science.1101141

Pedersen, T.H., F. de Paoli, and O.B. Nielsen. 2005. Increased excitability of acidified skeletal muscle: role of chloride conductance. *J. Gen. Physiol.* 125:237–246. doi:10.1085/jgp.200409173

Ranganathan, R., J.H. Lewis, and R. MacKinnon. 1996. Spatial localization of the K+ channel selectivity filter by mutant cycle-based structure analysis. *Neuron.* 16:131–139. doi:10.1016/S0896-6273(00)80030-6

Rychkov, G.Y., M. Pusch, D.S. Astill, M.L. Roberts, T.J. Jentsch, and A.H. Bretag. 1996. Concentration and pH dependence of skeletal muscle chloride channel ClC-1. *J. Physiol.* 497:423–435.

Saviane, C., F. Conti, and M. Pusch. 1999. The muscle chloride channel ClC-1 has a double-barreled appearance that is differentially affected in dominant and recessive myotonia. *J. Gen. Physiol.* 113:457–468. doi:10.1085/jgp.113.3.457

Scott, J.W., S.A. Hawley, K.A. Green, M. Anis, G. Stewart, G.A. Scullion, D.G. Norman, and D.G. Hardie. 2004. CBS domains form energy-sensing modules whose binding of adenosine ligands is disrupted by disease mutations. *J. Clin. Invest.* 113:274–284.

Steinmeyer, K., C. Ortland, and T.J. Jentsch. 1991. Primary structure and functional expression of a developmentally regulated skeletal muscle chloride channel. *Nature.* 354:301–304. doi:10.1038/354301a0

Tseng, P.Y., B. Bennetts, and T.Y. Chen. 2007. Cytoplasmic ATP inhibition of CLC-1 is enhanced by low pH. *J. Gen. Physiol.* 130:217–221. doi:10.1085/jgp.200709817

Wellhauser, L., H.H. Kuo, F.L. Stratford, M. Ramjeesingh, L.J. Huan, W. Luong, C. Li, C.M. Deber, and C.E. Bear. 2006. Nucleotides bind to the C-terminus of ClC-5. *Biochem. J.* 398:289–294. doi:10.1042/BJ20060142

Zhang, R., G. Evans, F.J. Rotella, E.M. Westbrook, D. Beno, E. Huberman, A. Joachimiak, and F.R. Collart. 1999. Characteristics and crystal structure of bacterial inosine-5′-monophosphate dehydrogenase. *Biochemistry.* 38:4691–4700. doi:10.1021/bi982858v

Zhang, X.D., P.Y. Tseng, and T.Y. Chen. 2008. ATP inhibition of CLC-1 is controlled by oxidation and reduction. *J. Gen. Physiol.* 132:421–428. doi:10.1085/jgp.200810023

Zifarelli, G., and M. Pusch. 2008. The muscle chloride channel ClC-1 is not directly regulated by intracellular ATP. *J. Gen. Physiol.* 131:109–116. doi:10.1085/jgp.200709899

Zifarelli, G., and M. Pusch. 2009. Intracellular regulation of human ClC-5 by adenine nucleotides. *EMBO Rep.* 10:1111–1116. doi:10.1038/embor.2009.159